EXTRACTION OF ACCURATE TIE POINTS FOR AUTOMATED POSE ESTIMATION OF CLOSE-RANGE BLOCKS

L. Barazzetti*, F. Remondino**, M. Scaioni*

* Politecnico di Milano, Department of Building Engineering Science and Technology, Milan, Italy
Email: (luigi.barazzetti, marco.scaioni)@polimi.it, web: http://www.best.polimi.it
** 3D Optical Metrology Unit, Bruno Kessler Foundation, Trento, Italy
Email: remondino@fbk.eu, web: http://3dom.fbk.eu

Commission III - WG 1

KEY WORDS: Feature Extraction, Matching, Orientation, Robust Estimation

ABSTRACT:
The article presents a powerful and automated methodology to extract accurate image correspondences from different kinds of close-range image blocks for their successive orientation with a bundle adjustment. The actual absence of a commercial solution able to automatically orient markerless image blocks confirms the still open research in this field. The developed procedure combines different image processing algorithms and robust estimation methods in order to obtain accurate locations and a uniform distribution of tie points in the images. We demonstrate the capabilities and effectiveness of this method with several tests on closed or open sequences and sparse blocks of images captured by a standard frame (pinhole) camera, but also spherical images. An accuracy evaluation of the achieved 3D object coordinates with photogrammetric bundle techniques is also presented.

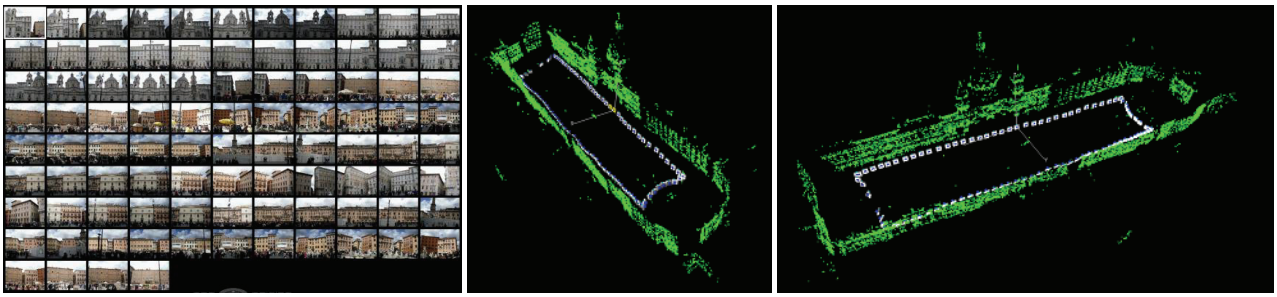

Figure 1. Typical sequence (92 images) automatically oriented extracting the necessary image correspondences (18,500 3D points).

1. INTRODUCTION

The complexity and diversity of the image network geometry in close-range applications, with wide baselines, convergent images, illumination changes, moving objects, occlusions, variations in resolution and overlap, makes the automated identification of tie points more complex than in standard aerial photogrammetry. Homologues image points are necessary for structure and motion determination, as well as 3D modeling purposes or Photosynth-like applications. In close-range photogrammetry, commercial solutions for automated image orientation and sparse 3D geometry reconstruction of markerless sets of images are still pending. Some commercial packages are available to automatically orient video sequences (e.g. Boujou, 2D3 and MatchMover, RealViz), but they generally work only with very short baselines and low resolution images. Thus, there is a lack of commercial and reliable software to automatically orient a set of unordered and markerless images. In the literature there are some approaches tailored to work in real-time and on large indoor or outdoor environments. These methods, typically named SLAM, can also use external information coming from exogenous sensors (e.g. GPS or IMU) for better incremental motion estimation and absolute geo-referencing (Davison *et al.*, 2007; Agrawal and Konolige, 2008; Pollefeys *et al.*, 2008).
When no assumption or external information are employed, the "Structure from Motion" (SfM) concept is the core method used for the automated orientation of images and 3D sparse reconstruction of scenes (Pollefeys and Van Gool, 2002). Nister (2004) matches small subsets of images to one other and then merge them for a complete 3D reconstruction in form of sparse point clouds. Vergauwen and Van Gool (2006) developed a SfM tool for Cultural Heritage applications (hosted now in a web-based 3D reconstruction service). Recently the SfM concept has made tremendous improvements, notwithstanding the achievable 3D reconstructions are useful only for visualization, object-based navigation, annotation transfer or image browsing purposes. However, the automation of the procedure has reached a significant maturity with the capability to orient huge numbers of images. Two well-known packages are Bundler (or its graphical version Photosynth) (Snavely *et al.*, 2008a) and Samantha (Farenzena *et al.*, 2009). The former is the implementation of the current state of the art for sequential SfM applications, and it was also extended towards a hierchical SfM approach based on a set of key-images (Snavely *et al.*, 2008b). The latter appears even faster because of the introduction of a local bundle adjustment procedure.
In the photogrammetric community, some research solutions capable of automatically orienting a set of markerless images acquired with calibrated cameras were presented in Roncella *et al.* (2005), Läbe and Förstner (2006) and Remondino and Ressl (2006). A rigorous bundle solution, coupled with the estimation of the unknown parameters based on the Gauss-Markov model of the Least Squares, provided an efficient, precise and reliable solution in a functional and stochastic sense.
The paper presents a methodology for the automated identification of image correspondences in a large variety of image datasets (Figure 1). The proposed method, named with

the acronym ATiPE (Automatic Tie Point Extraction), is distinguished from previous works for its flexibility, completeness of the achieved sparse point clouds and capability to process different types of images. The robust detection of correspondences is achieved by combining the accuracy of traditional photogrammetric methods with the automation of Computer Vision (CV) approaches. The method has been implemented into a software which is capable of interacting and transferring data with several commercial photogrammetric packages for the successive bundle adjustment. Many tests have been performed in order to validate the methodology on different datasets acquired with pinhole cameras as well as on spherical images. Results obtained from some of them will be shown in Section 3.

2. WORKFLOW OF ATIPE

2.1 Overview of the methodology

The developed method (ATiPE) can automatically process a large variety of images, in order to derive accurate correspondences for the successive estimation of camera poses and sparse 3D geometry. ATiPE was designed for photogrammetric and detailed 3D modeling applications, therefore a real-time elaboration is not an issue of primary importance in favour of the final accuracy and uniform distribution of the extracted tie points. The implemented feature matching strategies, coupled with an initial network geometry analysis (called *visibility map*), allows a computational time of few hours for image blocks composed of several tenth of high resolution images (> 20 Megapixel) used at their original size. The typical output of ATiPE are the pixel coordinates of homologues image points, which can be imported and used for image orientation and sparse geometry reconstruction in most commercial photogrammetric software (e.g. LPS, Australis, iWitness, iWitnessPro, PhotoModeler). The innovative aspects of ATiPE are:

- effectiveness on a large variety of unorganized and fairly large pinhole camera image datasets;
- capability of working with high resolution images;
- accurate image measurements based on the *Least Squares Matching* (LSM);
- combination of *feature-based* and *area-based* operators;
- strategies to derive a uniform distribution of tie points in the images;
- extension to spherical images.

A comparison between ATiPE and the state-of-the-art Photo Tourism (e.g. Bundler or Photosynth) is given in Table 1. The flowchart of the method is shown in Figure 2, while details about the implemented procedure will be discussed in next paragraphs of this section. The input elements of ATiPE are the *images*, the full set of *interior orientation parameters* (optional) and a *visibility map* between the images (optional). The images are preferably used calibrated in order to avoid self-calibration which is generally not appropriate and reliable in practical 3D modelling projects due to the weak image network for a complete and correct camera calibration. The images can be radiometrically enhanced with the Wallis filter (1976), in the case of a poor texture. ATiPE follows a coarse-to-fine strategy in order (i) to work with the original geometric and radiometric resolution at the highest pyramid level and (ii) to speed up the processing. The *visibility map* might contain information about the overlap between the images and it can be derived from GPS/INS data with an approximate DTM/DSM or with a preliminary and very fast orientation procedure performed on low resolution images (e.g. 2 Megapixel). The visibility map can significantly reduce the running time of ATiPE by limiting the combination of images that must be analysed and matched.

	Photo Tourism	**ATIPE**
Purpose	CV Applications	Photogrammetric Surveys
Kind of Images	Pinhole	Pinhole & Spherical
Number of images	Huge (>10 000)	Limited (a few hundreds)
Varying cameras	Yes	Yes
Image size	Low resolution (compression)	High resolution with a coarse-to-fine approach
Image enhancement	None	Yes (Wallis filter)
Network geometry	Sparse block	Ad-hoc procedures for sparse blocks and sequences
Visibility information	None	Yes (images, GPS/INS, DTM/DSM)
Accuracy	No guarantee	Yes – using images for photogrammetric projects
Speed	Fast	Slow
Camera calibration	EXIF	EXIF or Interior with additional parameters
Operator for matching	SIFT	SIFT - SURF - FAST
Detector Comparison	kd-tree	Quadratic or kd-tree
Outlier Rejection	**F**/**E** matrix	**F**/**E** matrix or homography
F/**E** estimation	8-points	7-points
Robust method	RANSAC	LMedS - RANSAC – MAPSAC
Image coordinates refining	None	LSM
Additional image points	None	Multi-image corner-based matching
Tie point reduction	None	Yes
Tie point uniform distribution	None	Yes

Table 1. Comparison of the Photo-Tourism approach (Bundler - Photosynth) and ATiPE.

2.2 Feature detection and matching

A generic block of n images can be considered composed of $(n^2-n)/2$ combinations of stereo-pairs, which are firstly analysed independently for the identification of the correspondences and then progressively combined. For each pair, features are extracted with the SIFT (Lowe, 2004) or SURF (Bay *et al.*, 2008) operators, which demonstrated their high repeatability for close-range applications. The user needs to select the operator and the method for comparing the descriptors of the image points. Two methods are available: a *kd-tree* search (Arya, 1988) (fast but approximate) or a *quadratic* search (slow but rigorous). The use of the former is highly suggested in the case of high resolution images as it can extremely reduce the computational costs. The latter approach analyses all descriptor combinations and is surely more precise despite the slower performances. Thus, it should be used only in the case of low textured objects and highly convergent images. In both comparison methods, the *ratio test* on the L2 norm of the descriptors is applied for a preliminary outlier removal. The remaining wrong correspondences are removed with the robust estimation of the fundamental matrix (or essential matrix if interior orientation of the camera is known). Three methods have been implemented: LMedS, RANSAC and MAPSAC. None of these methods can be successfully applied to all kind

of datasets and every method has advantages and drawbacks with results depending on the selected thresholds and the expected fraction of outliers among the observations. Until now, the user has to manually select the outlier rejection method but a criterion for automatic switching on the basis of the detected characteristics is under development.

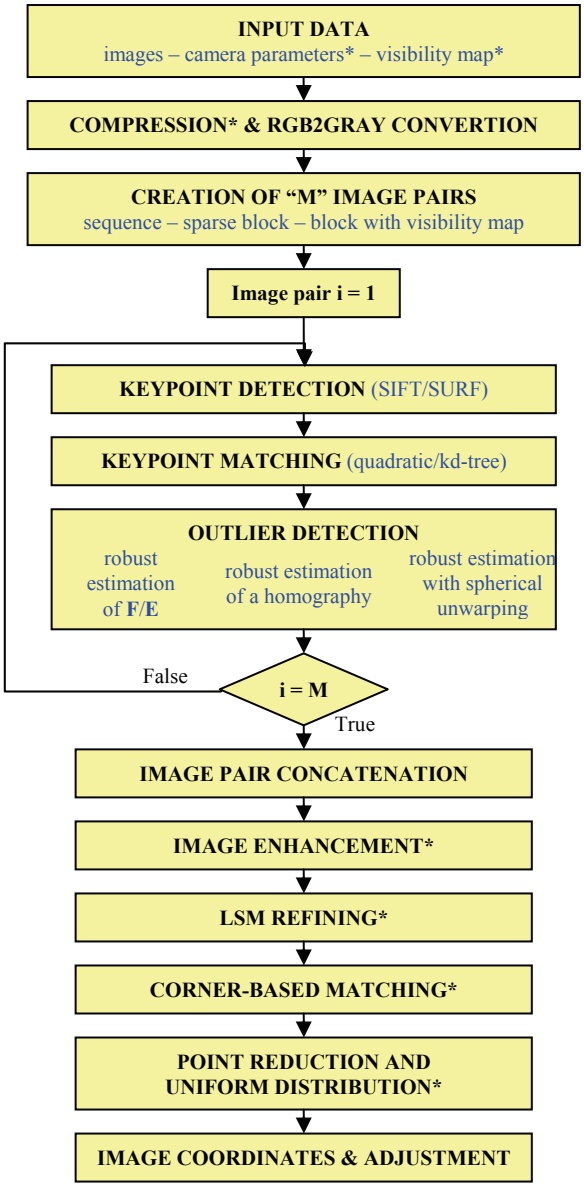

Figure 2. The flowchart of the implemented method. The "*" symbol indicates optional functions or data.

After the image pair matching for all possible combinations, the found stereo pairs are concatenated according to the network geometry. Different strategies can be followed:
- *ordered image sequences* (Figure 4 and 5)*:* as the overlapping is guaranteed between consecutives images, the whole sequence is divided into n-2 triplets. If I is a generic image, each triplet T_i is made up with the images $\{I_i, I_{i+1}, I_{i+2}\}$. For each triplet T_i a pair-wise matching between the couples of images $C_i = \{I_i, I_{i+1}\}$ and $C_i''=\{I_{i+1}, I_{i+2}\}$ is carried out in order to determine a set of homologous features. Correspondences of the couple $C_i'= \{I_i, I_{i+2}\}$ are determined from the points of the images I_{i+1} which also appear on the images I_i and I_{i+2}. After the single triplet matching, the image coordinates of consecutives triplets are compared in order to determine correspondences in the whole sequence. The triplet T_i and the next one $T_{i+1}= \{I_{i+1}, I_{i+2}, I_{i+3}\}$ share two images and their tie points can be transferred with a simple comparison based on the value of the image coordinates. In addition, for closed sequences an additional triplet $T_a=\{I_{n-1}, I_n, I_1\}$ is added to match first and last images. This method has a linear computational cost O(n) with respect to the number of images, with a significant advantage in terms of CPU time.
- *unordered sets of images* (Figure 6): this is the general case, where it is necessary to check all possible image pair combinations to determine the ones sharing sufficient correspondences. Therefore each image must be compared with all the others, leading to a high computational cost O(n^2). For this reason, the use of a *visibility map* (which can be automatically estimated) is recommended.

2.3 Image coordinates refinement

After the concatenation step, the precision of the image coordinates can be improved with a *Least Squares Matching* refining (LSM; Grün, 1985). Although an orientation with SIFT or SURF features can produce sub-pixel results, the refinement with LSM gives better results (Table 2). The use of LSM allows the analysis of low resolution images with SIFT and SURF (by using a coarse-to-fine approach). This limits the number of extracted features and speeds up the comparison of the descriptors. These features are then projected onto the original images by considering the applied compression factor and become good approximations for the LSM refining. In the case of widely separated and convergent images, the descriptor values can be used as initial approximation of the LSM parameters (Remondino and Ressl, 2006).

	Case1 (1936×1296 px)			*Case 2 (2816×2112 px)*		
	σ_0	RMS	#	σ_0	RMS	#
SIFT alone	0.54	0.36	87	1.21	0.86	793
SIFT+LSM	0.33	0.22	68	0.86	0.61	784
SURF alone	0.86	0.58	137	0.47	0.33	104
SURF+LSM	0.51	0.34	104	0.35	0.24	95

Table 2. Orientation results in terms of σ_0, RMS (both in pixels) and number of final 3D points with the SIFT and SURF operators, coupled with an image location improvement (LSM).

	6 images - 2816×2112 (px) Object size: 1.2×1×1 (m)	
	SIFT+LSM	FAST+LSM
#3D points	1181	541
σ_0 (px)	0.42	0.28
RMS (px)	0.43	0.32
σ_x (mm)	0.27	0.13
σ_y (mm)	0.39	0.24
σ_z (mm)	0.65	0.33

Table 3. Comparison between feature- and corner-based orientation procedures with a LSM refining.

As the precision of the computed object coordinates improves with the number of images where the same point is visible, an additional matching procedure based on the FAST operator (Rosten and Drummond, 2006) was added. FAST demonstrated to quickly extract a large number of corners under a higher repeatability compared to SIFT and SURF, with also a better distribution in the images and a higher accuracy of the final sparse geometry (Jazayeri and Fraser, 2008). According to these considerations, the FAST operator was included in the pipeline

(as optional choice). Its interest points are matched with a multi-image geometrically constrained LSM (Grün and Baltsavias, 1988) based on the collinearity principle and the orientation parameters previously computed with SIFT or SURF features. Table 3 shows the accuracy improvement using the developed approach.

2.4 Correspondence reduction and uniform distribution

High resolution images picturing objects with a good texture could generate a huge number of image correspondences, which are very often not uniformly distributed in the images. Therefore, each image can be divided into rectangular cells where only the features with the largest multiplicity are held. This method demonstrated a significant reduction of the correspondences (even more than 100 times), preserving the accuracy of the final product. Secondly, as the features are generally random-distributed in the images without a uniform distribution (Figure 3), the method improves the geometric distribution of tie points. The quality of the final results is increased in terms of geometric distribution of tie points and in a drop of the processing time and computational cost.

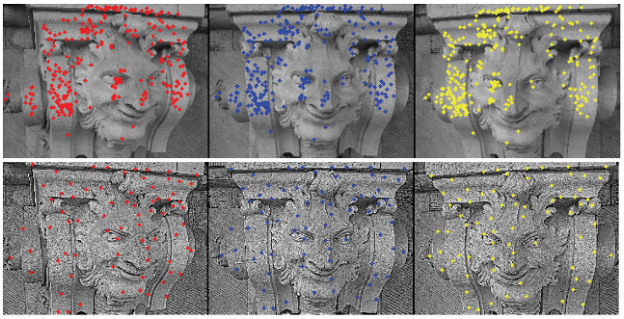

Figure 3. Random and non-uniform distribution of the features extracted with SIFT (above) and derived uniform distribution with the proposed approach (below).

2.5 Extension to spherical images

ATiPE can be also used to extract reliable correspondences from *spherical images* (or *panoramas*), i.e. a mosaic of separated images acquired with a rotating head and stitched together. The derivation of metric information from spherical images for interactive exploration and realistic 3D modeling is indeed receiving great attention due to their high-resolution contents, large image field of view, low cost, easiness, rapidity, and completeness (Fangi, 2007). But spherical images, if unwrapped on a plane, feature different resolutions (width and height), scale changes and the impossibility to use a classical bundle solution in Cartesian coordinates. In fact, while a pinhole image is described by its camera calibration parameters, a generic spherical image is only described with its circumference C, which corresponds to the image width (in pixels) under an angle of 2π. In fact, a spherical image can be intended as a unitary sphere S around the perspective centre and 3D point coordinates $\mathbf{x}$ can be expressed in terms of longitude λ and co-latitude ψ as:

$$\mathbf{x} = \begin{bmatrix} x & y & z \end{bmatrix}^T = \begin{bmatrix} \sin\psi\cos\lambda & \sin\psi\sin\lambda & \cos\psi \end{bmatrix}^T \quad (1)$$

The relation between a point onto the sphere and its corresponding 3D coordinates is $\mathbf{x} = \mathbf{X} / \| \mathbf{X} \|$. Homogenous image coordinates $\mathbf{m}$ can be mapped onto the sphere by using the *equi-rectangular* projection:

$$\mathbf{m} = \begin{bmatrix} m_1 & m_2 & 1 \end{bmatrix}^T = \begin{bmatrix} R\lambda & R\psi & 1 \end{bmatrix}^T \quad (2)$$

where $R=C/(2\pi)$ is the radius of the sphere.
Given a spherical image, we developed a matching strategy to unwrap the sphere onto a local plane. First of all, the median of the longitudes $\mu(\lambda)$ is subtracted from λ, obtaining new longitudes $\lambda^* = \lambda - \mu(\lambda)$. This allows the projection of the points of the sphere onto the plane $x = 1$ as:

$$\mathbf{p} = \begin{bmatrix} 1 & p_2 & p_3 \end{bmatrix}^T = \begin{bmatrix} 1 & tg\lambda^* & \cot\psi / \cos\lambda^* \end{bmatrix}^T \quad (3)$$

Here, p_2 and p_3 can be intended as the inhomogeneous image coordinates of a new pinhole image. Moreover, the centre of the spherical images is also the projection centre of the new pinhole image, with the advantage that given two spherical images S and S', an outlier can be removed by robustly estimating a fundamental matrix. Obviously, this procedure cannot cope with large longitude variations. However, the partitioning of the spherical images into 4 zones ($k\pi/2 \le \lambda < (k+1)\pi/2$, $k = 0,\ldots, 3$) produces 4 local pinhole images that can be independently processed. In addition, this method allows the combined matching of spherical and pinhole images.
The extracted image correspondences are then processed with a bundle solution in spherical coordinates to derive the camera poses and a sparse 3D geometry of the analyzed scene.

3. EXPERIMENTS

3.1 Ordered image sequences

Figure 4a shows the recovered poses for a sequence matched with the SIFT operator and the *kd-tree* search for comparing its descriptors. It took roughly 30' to orient 33 images (used at their original size) acquired with a 10 Megapixel calibrated camera. The robust estimation of the epipolar geometry was necessary to remove mismatches (e.g. moving objects such as people and pigeons). The orientation procedure was carried out starting with a relative orientation between the first image pair, then progressive resections alternated to triangulations have been used to provide approximations for the final and robust photogrammetric bundle adjustment. Figure 4b shows the poses of 28 images recovered with the SURF operator in 15', deriving a final sparse point cloud of ca 12,000 3D tie points.
Figure 5 shows the results from the ISPRS Comm. 3 dataset "Fountain-K6". The 25 images have been automatically oriented with the SIFT operator in approximately 20'. The adjustment with all the extracted features (more than 96,000 image points) gave a final RMS of 3.6 µm, while the application of the point reduction described in subsection 2.4 (ca 6,000 image points) ended with a RMS of 3.3 µm.

3.2 Sparse image block

ATiPE has been also tested on large image blocks acquired with an UAV system. Figure 6 shows the orientation results for a block of 70 images taken with a calibrated 12 Megapixel camera. The global number of image combination is 2,415, while the pre- analysis with the visibility map found 507 image combinations.

Figure 4. Orientation results for closed and ordered image sequences acquired with a 10 Megapixel calibrated camera. a) 33 images; b) 28 images.

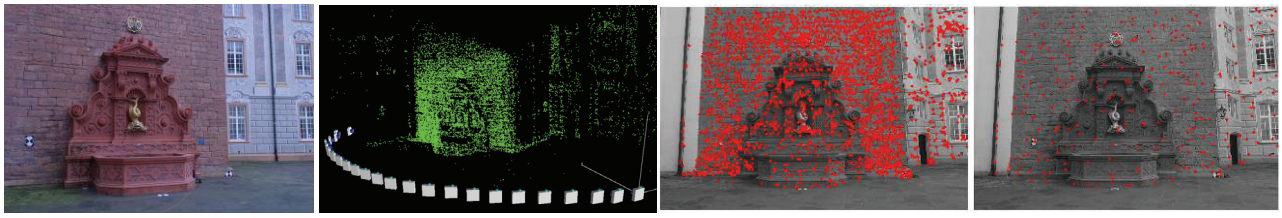

Figure 5: The dataset "Fountain-K6" (from ISPRS Comm. 3) automatically oriented with ATiPE. The results of the procedure to reduce and obtain a more uniform distribution of the tie points are also shown on the right side.

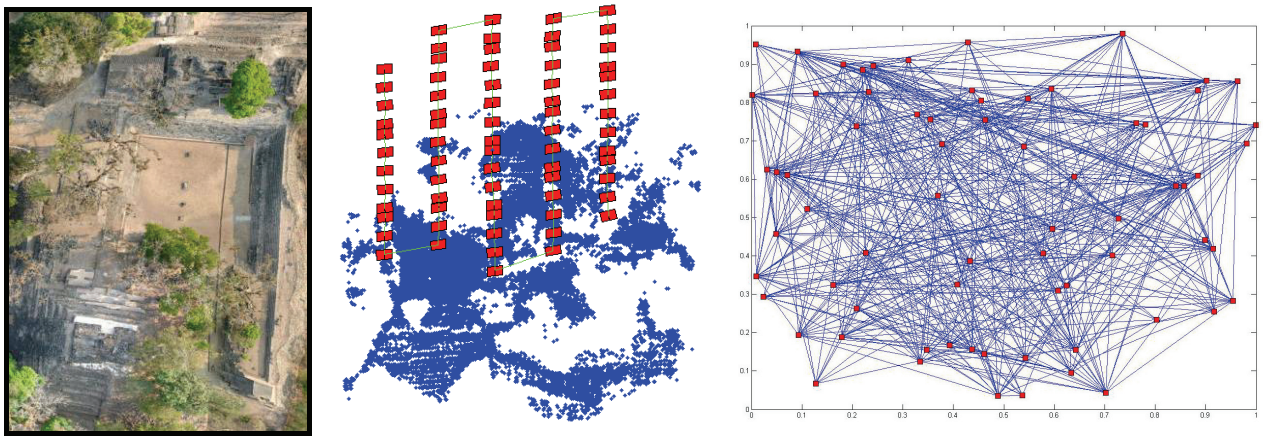

Figure 6. Recovered camera poses and sparse 3D geometry for a block of 70 UAV images over the archaeological area of Copan, Honduras. A mosaic of the images and the *visibility map* (red points represent image locations and blue lines connections among them) are also shown.

At the end of the *feature-based* matching, more than 57,000 image points have been found (only correspondences in at least three images have been kept). The final photogrammetric bundle adjustment provided a RMS of 3.4 μm (pixel size is 5.5 μm). After the strategy for point reduction and uniform distribution, only 6,498 correspondences have been used to derive the camera poses with a final RMS of 3.1 μm.

3.3 Spherical images

ATIPE has been also used to register very large panoramas obtained by stitching together frame images with panoramic software (e.g. PTGui). Figure 7 shows the matched features between 3 panoramas in Petra (ca 80-90 Megapixel per image). The façade is approximately 70x40 m and the camera-to-object distance was about 70 m. Around 1,600 correspondences have been found and then used to retrieve the camera poses with a bundle adjustment in spherical coordinates (Fangi, 2007). The final standard deviations of the computed camera poses are 4-5 cm, in agreement with the values derived from manual measurements.

Figure 8 shows the tie points extracted between two widely separated panoramas (covering an horizontal angle of 270°), employed for the successive image orientation and 3D scene restitution of a block of 16 panoramas. It is clearly visible how the method can work even with large topological changes.

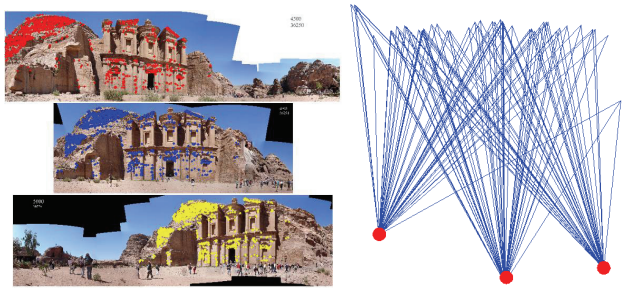

Figure 7. A triplet of spherical images with the extracted correspondences for the successive bundle adjustment.

4. CONCLUSIONS

This paper presented an accurate and powerful methodology to extract precise and reliable image correspondences for camera pose estimation and 3D sparse geometry derivation. The method was tested on pinhole and spherical images, large and small blocks, low and high resolution images.

The implemented tool was created for photogrammetric applications, in which accuracy plays a fundamental role. It uses several CV techniques, which are mixed with the photogrammetric ones to bring accuracy into automation. In addition, some new methods were developed and implemented to overcome some issues related to the distribution and number of the image correspondences: (i) a coarse-to-fine approach allows the elaboration of high resolution images; (ii) an implementation of strategies to reduce the number of the images to be pair-wise matched; (iii) according to the block structure, a *kd-tree* or a *quadratic* search and the preliminary creation of a *visibility map* are applied; (iv) a method for tie points reduction to avoid too large datasets of observations for the successive bundle adjustment. These solutions demonstrated to reduce both processing time and computational costs without loosing accuracy.

The final results are accurate tie points between different categories of images that can be used for the camera estimation phase within a robust Gauss-Markov bundle adjustment.

Figure 8. Two panoramas (out of 16, ca 120 Megapixel per image) of the interior of S.Maria della Carità church in Italy and the extracted tie points. Some lines are drawn to indicate the correct correspondences extracted despite the large disparities in the images.

REFERENCES

References from Journals:

Agrawal, M., Konolige, K., 2008. FrameSLAM: from Bundle Adjustment to Realtime Visual Mapping. *Trans. on Robotics*, 24(5), pp. 1066-1077.

Arya, S., Mount, D.M., Netenyahu, N.S., Silverman, R., Wu, A.Y., 1988. An optimal algorithm for approximate nearest neighbour searching fixed dimensions. *Journal of the ACM*, 45(6), pp. 891-923.

Bay, H., Ess, A., Tuytelaars, T., Van Gool, L., 2008. SURF: Speeded up Robust Features. *CVIU*, 110(3), pp. 346-359.

Davison, J., Reid, I., Molton, N., Stasse, O., 2007. MonoSLAM: Real-time single camera slam. *IEEE PAMI*, 29(6), pp. 1052-1067.

Grün, A., 1985. Adaptative Least Squares Correlation: a powerful matching technique. *South African J. of Photogrammetry, Remote Sensing and Cartography*, 14(3), pp. 175-187.

Grün, A., Baltsavias, E.P., 1988. Geometrically constrained multiphoto matching. *PE&RS*, 54(5), pp. 633-641.

Lowe, D., 2004. Distinctive image features from scale-invariant keypoints. *IJCV*, 60(2), pp. 91-110.

Pollefeys, M., Van Gool, L., 2002: From images to 3D models. *Communications of the ACM*, 45(7), 50–55.

Pollefeys, M., Nister, D., Frahm, J. M., Akbarzadeh, A., Mordohai, P., Clipp, B., Engels, C., Gallup, D., Kim, S. J., Merrell, P., Salmi, C., Sinha, S., Sinha, S., Talton, B., Wang, L., Yang, Q., Stewenius, H., Yang, R., Welch, G., Towles, H., 2008: Detailed real-time urban 3D reconstruction from video. *IJCV*, 78(2-3):143–167.

Snavely, N., Seitz, S.M., Szelinski, R., 2008a. Modelling the world from internet photo collections. *IJCV*, 80(2), pp. 189-210.

Vergauwen, M., Van Gool, L.J, 2006. Web-based reconstruction service. *Machine Vision and Applications*, 17(6), pp. 411-426.

References from Other Literature:

Fangi, G., 2007. The Multi-Image Spherical Panoramas as a Tool for Architectural Survey. Proc. of XXI Int. CIPA Symposium, Athens.

Farenzena, M., Fusiello, A., Gherardi, R., 2009. Structure and Motion pipeline on a hierchical cluster tree. Proc. IEEE 3DIM, Kyoto, Japan.

Jazayeri, I., Fraser, C., 2008. Interest operators in close-range object reconstruction. *IAPRSSIS*, Vol. 37, Part V/1, pp. 69-74.

Labe, T., Förstner, W., 2006. Automatic relative orientation of images. In: Proc. of the 5th "Turkish-German Jount Geodetic Days", 6 pp.

Nister, D., 2004. Automatic passive recovery of 3D from images and video. In: proc. of the 2nd IEEE Int. Symp. on "3D data processing, visualization and transmission", pp.438-445.

Remondino, F., Ressl, C., 2006. Overview and experience in automated markerless image orientation. *IAPRSSIS*, Vol. 36, Part 3, pp. 248-254.

Roncella, R., Forlani, G., Remondino, F., 2005. Photogrammetry for geological applications: automatic retrieval of discontinuities in rock slopes. Proc. Videometrics VIII, SPIE IS&T Electr. Imaging, pp. 17-27.

Rosten, E., Drummond, T., 2006. Machine learning for high speed corner detection In: Proc. of of the European Conf. on Computer Vision, Graz, Austria, pp. 430-443.

Snavely, N., Seitz, S.M., Szelinski, R., 2008b. Skeletal sets for efficient Structure from Motion. Proc. CVPR2008, 11 p.

Wallis, R., 1976. An approach to the space variant restoration and enhancement of images. In: Proc. of Symp. on "Current Mathematical Problems in Image Science", pp. 329-340.